# Function Representation for Robotic 3D Printed Concrete

Shajay Bhooshan[1,2(✉)], Johannes Ladinig[3,4], Tom Van Mele[1], and Philippe Block[1]

[1] Institute of Technology in Architecture, Block Research Group, ETH Zurich, Stefano-Franscini-Platz, HIB E 45, 8093 Zurich, Switzerland
bhooshan@arch.ethz.ch
[2] Zaha Hadid Computation and Design Group, London, UK
[3] Incremental 3D, Innsbruk, Austria
[4] Structure and Design, Institute of Design, University of Innsbruck, Innsbruck, Austria

**Abstract.** The use of Function Representation (FRep) to synthesise and specify geometries for 3D printing is finding renewed interest. The usefulness and extension of this representation in the synthesis and analysis of geometries for the process of large-scale, layered concrete 3D printing has been previously articulated by the authors. This paper fully extends the implicit representation used previously in shape-design to fabrication-related processing of compressive skeletal structures for realisation by robotic 3D printing of concrete. In particular, we use an initial value formulation of a propagating front to process the nodes and bars of a given funicular spatial structure.

**Keywords:** 3D printing · Implicit modelling · Function representation
Shape design · Funicular skeletons · Robotic concrete printing

## 1 Introduction

The use of Function Representation (FRep) to synthesise and specify geometries for 3D printing is finding renewed interest (Keeter 2013; Lu et al. 2014). The extension of this representation for the synthesis and analysis of geometries for layered process of large-scale concrete 3D printing has been previously articulated by the authors (Bhooshan et al. 2018). The shape-design framework described there is motivated by the rapid growth in large-scale, robotic 3D printing and lack of appropriate shape-design tools. Further, the framework is based on a novel insight regarding the applicability of design methods used in unreinforced, compressive masonry to layered 3D printing with materials of relatively low tensile capacity such as concrete. This paper further extends the FRep, used previously in shape-design, to fabrication-related processing of geometries. In particular, the framework is applied to process compressive skeletal structures for realisation by concrete printing. Lastly, physical results demonstrating the application are shown.


J. Willmann et al. (Eds.): ROBARCH 2018, *Robotic Fabrication in Architecture, Art and Design 2018*, pp. 98–109, 2019.
https://doi.org/10.1007/978-3-319-92294-2_8

### 1.1 Compressive Skeletal Structures and 3D Printing

Skeletal structures are commonly realised in steel and timber (Rian and Sassone 2014). Historically, they have also been realised in stone, prominently at the Sagrada Familia cathedral in Barcelona. Their realisation in cast concrete is perhaps most famously executed by Architect-Engineer Luigi Nervi (Perugini and Andreani 2013) and Engineer Robert Malliart (Zastavni 2008). However, the use of concrete for their realisation is nowadays often hindered by the high cost associated with the use of custom-tailored moulds and formwork (West 2001). There have been some efforts to alleviate this short-coming with the use of knit and fabric formworks (Popescu et al. 2016; West 2016). Of relevance to the current discussion however, are recent developments in the use of large-scale 3D printing with concrete to produce such skeletons. These efforts are currently restricted to the production of outer casings into which regulation-approved concrete is subsequently poured (XtreeE 2017).

### 1.2 Contributions and Outline

In considering a shape representation that is appropriate for both design and fabrication processing of skeletal shapes for concrete printing, we may highlight the following: (1) An ideal shape representation includes both the centre-lines of structural action and the layers of printing; (2) the shape representation makes no or little *a priori* assumptions regarding the topological complexity of the skeletal networks; and (3) the shape representation is amenable for fabrication-related processing addressing the particular constraints of concrete 3D printing such as heuristics related to maximum overhang, preferably planar assembly interfaces etc. The main contributions of this paper relate to outlining the extension of our FRep-based framework to address the first two aspects above (Sect. 3.1), whilst detailing its application to address the third (Sects. 3.2 and 3.3).

## 2 Related Work

Given the dual intention of both previous and current work, to support interactive and exploratory shape design whilst ensuring adequate representation of critical fabrication-related aspects, relevant domains of precedent work include the areas of computer graphics and computer-aided-geometric-design (CAGD). Medical imaging with its history of representing topologically complex and solid 3D shape via a stack of 2D images resonates with the requirements of representing the process of layered 3D printing of concrete. It thus provides another rich, if unusual, domain of precedent work.

### 2.1 3D Printing and Implicit Shape Representation

Implicit representation has widespread use in various domains including design and animation of articulated characters (Ji et al. 2010), modelling of biological shapes (Sherstyuk 1999a), computer-aided-design (Rossignac 1985), physically based animation (Desbrun and Gascuel 1995), rendering of fonts (Green 2007) etc. However, to

the best of our knowledge, their use has not yet been adapted to synthesise shapes for concrete printing, apart from our previous work and its application by our collaborators (Bhooshan et al. 2018).

All forms of implicit representation share the following advantages (Opalach and Maddock 1995): (1) efficient to check for whether a given point is inside or outside the object, (2) efficient boolean operations, (3) easy-to-make topological changes, (4) efficient blending between objects, etc. We thus believe it is a natural representation scheme to be adapted for shape design for robotic and layered 3D printing of concrete, as well as its fabrication-related processing.

### 2.2 Implicit Modelling

In implicit representations, the shape of an object is represented by defining a scalar field (also called potential field or field function) that assigns positive values to points in the field that are outside the represented object and negative values for those inside. Thus, the surface of the object is implied as the boundary between the inside and outside of the object so represented. Technically, the surface of the object is the zero iso-surface of the scalar field. In contrast, Boundary Representations (BRep) parametrically define the surface of the object. For more on implicit surfaces, we refer the reader to the seminal paper by Bloomenthal and Bajaj (1997).

### 2.3 Skeleton Based Implicit Modelling and Function Representation

Given the requirements of the shape representation in relation to and its manipulation via a skeletal, centre-line graph of vertices and edges, skeleton-based implicit modelling becomes relevant precedent work (Bloomenthal and Shoemake 1991; Sherstyuk 1999a). Here, the scalar fields are defined in relation to the distance from a given skeletal graph with distances on the inside of the object being negative and those outside positive. Thus, sometimes a related terminology of signed distance fields (SDF) is used in this context (Hubert and Cani 2012). Lastly, various models of implicit representations are unified into the so-called Function Representation (FRep) (Pasko and Adzhiev 2002).

### 2.4 Medical Imaging and Layered Printing

The trajectories that the print head of the 3D printer has to traverse - the so-called task graphs (Khoshnevis et al. 2006) – are usually generated by processing BRep surfaces (Fig. 1). Alternatively, the layered process of 3D printing, like brick masonry, can be considered as advancing or propagating ground-upwards, one layer at a time. Furthermore, this view is particularly instructive in understanding the stability of the layers whilst printing, apart from foregrounding the layers themselves as opposed to the geometry from which they are derived. In this context, precedent work from the field of medical imaging becomes relevant. Front propagation or advancing front can be modelled as a parametrically represented boundary curve that evolves in time (boundary value formulation) or as the zero iso-contour of a scalar field that itself moves or evolves through time (initial value formulation) (Kass et al. 1988; Sethian 1998). Both methods

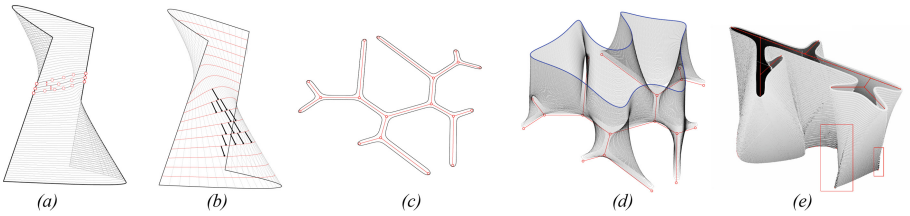


**Fig. 1.** Processing of mesh representation to generate (a) horizontal and (n) field-aligned task graphs.

are used in medical imaging to recover shapes from a stack of 2D images. This approach has also been recently used to minimise the amount of support structures required for overhanging parts in 3D printing and architecturally, to recreate the columns of Sagrada Familia (Cacace et al. 2017; Monreal 2012).

### 2.5 Previous Work

The authors have previously articulated and utilised the boundary value formulation to model and realise shapes in 3D Printed concrete (Fig. 1(c, d)). However, such parameterised boundary representations encounter difficulties when the curve expands or shrinks along its normal field and sharp corners and cusps develop or pieces of the boundary intersect (Cohen 1991). This can be seen in some of our previous results (Fig. 1(e)).

## 3 Processing of Funicular Networks for Concrete Printing

In comparison to previous work (Sect. 2.5), in the current work and paper, we utilise the alternative, initial value formulation and adapt it to model the layered geometries of concrete 3D printing. In particular, we combine them with a skeletal graph representation of 3D funicular networks to process them for physical realisation.

### 3.1 3D Skeletons and Initial Value Formulation of Front Propagation

It would be possible to use a BRep-based approach to process nodes and bars for 3D printing via the procedural thickening of the skeletal graph and subsequent contouring of the meshes that represent nodes and bars of the network (Fig. 2(a–d)). However, such geometric processing of nodes and bars increase in complexity when processing nodes requiring overhang support and/or with increased topological complexity. This approach holds further complications with regard to assignment of ideal print directions to the node in addition to resolving complex interfaces between the print layers of the nodes and bars (Fig. 2). Furthermore, local processing of print layers does not guarantee good alignment with the funicular force flow over the node.

Our approach, on other hand, capitalises on the rich and easy-to-implement operation set of FRep to alleviate this complexity, easily handle topological changes from

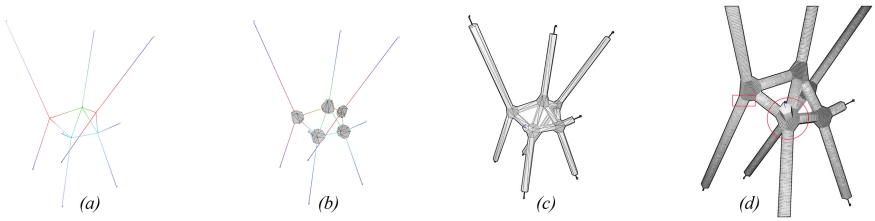


**Fig. 2.** (a–c) Generating convex hulls around nodes and bars of a graph, (c) contouring the combined mesh. Alignment and interface problems with task graphs.

one print layer to another, naturally specify interior task graphs (printing paths) that add stability to the print and more importantly directly model the task graphs and their evolution in time (Fig. 3).

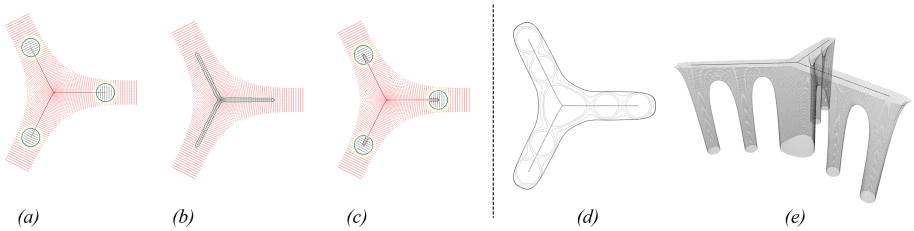


**Fig. 3.** (a) and (b) two scalar fields. (c) set-theoretic difference operation of (b) on (a). (d) the natural extension of specifying interior task graphs as contours of a scalar field, (e) Natural handling of topological change of many closed curves at the bottom layer to a singular closed curve on the top layer.

### 3.2 Primitive Field Functions and Operations

There are wide varieties of field functions that have been developed to adapt the use of Function Representation within various application domains. We currently use two simple-to-implement, two-dimensional SDF functions and their booleans, blends and evolution along a normal direction to generate the task graphs. The first field function is the so-called soft-objects field function (Wyvill et al. 1986), which is specified in relation to distance of field points from the nodes of an input graph (Fig. 4(a)). The other field function uses the same function, albeit in relation to the shortest distance from the field point to each of the edges of a 2D input graph (Fig. 4(b)). These simple functions may be replaced by more involved convolution field functions that improve the short-comings of these simple functions (Sherstyuk 1999b; Wyvill and Wyvill 1989).

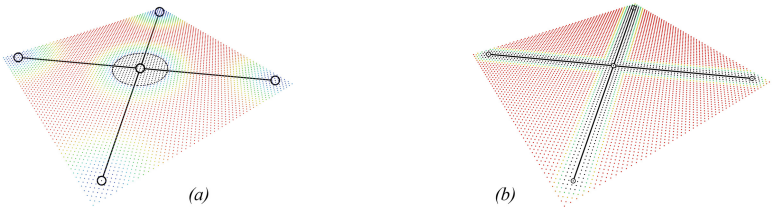


**Fig. 4.** (a) Signed distance fields (SDF) in relation to (a) nodes and (b) edges of a skeletal graph.

### Booleans

We use standard set-theoretic definitions to specify the Union, Difference and Intersection between two scalar fields (Bloomenthal and Bajaj 1997) (Fig. 5(a–e)).

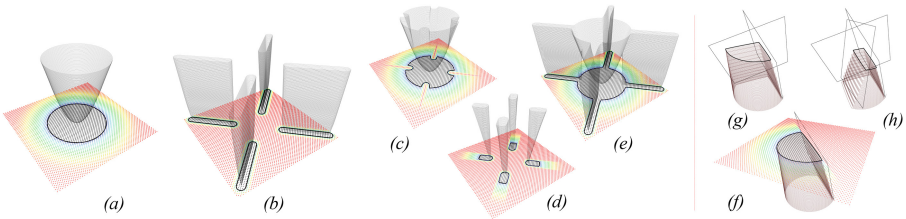


**Fig. 5.** (c) Difference, (e) Union and (d) Intersection operations on primitive fields (a) and (b). (f) Consequence of trim operation on the scalar field. (h) (g) trim operations can be successively applied.

### Trim with Plane

When we use a trim operation using an input plane, we replace the field values of all field points that are on the negative side of the plane (w.r.t its normal) with a value of 1 (Fig. 5(f–h)). In other words, all points on the negative side of the plane are considered outside the object. We use this operation primarily to aid the assembly of printed parts or interface between parts that are consecutively printed (while the first part is still wet).

### Blend

We currently use a simple linear additive interpolation function between two given scalar fields to specify a blend (Fig. 6(a and b)). It is common to use the so-called smooth step function to improve the behaviour of the blend at the extremes.

## 3.3 Processing Nodes

Each of the nodes is printed separately. However, the parts of every node are printed consecutively whilst the previous part is still wet, enabling a material bond across the node. In terms of the processing of the node, this does not pose any additional difficulty.

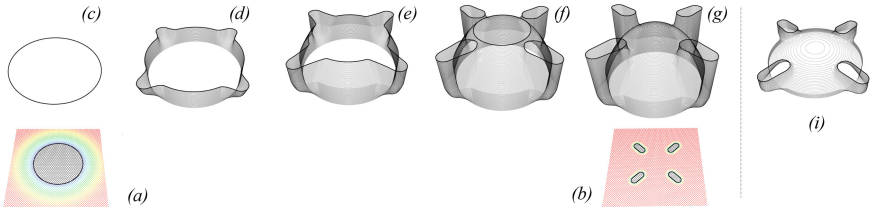


**Fig. 6.** (c–g) Blend sequence of the zero contour as scalar field (a) blends to scalar field (b). The effect of a faster blend rate on the shape of the geometry described by the stack of zero-contours is shown in (i).

The simplest procedure to produce the task graphs is by translating a circular front along the edge, and simultaneously trimming against the bisector planes defined between pairs of edges (Fig. 7(a)). In other words, in this simple method, the front does not really evolve.

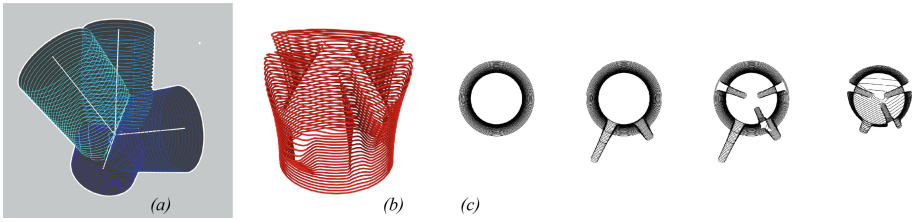


**Fig. 7.** A nominal procedure of translate and trim to synthesise task graphs for each node segment. (b) Task graphs of one of the four parts meeting at node shown in Fig. 10.

In most practical cases on the other hand, the moving front needs to evolve features to ease steep overhangs and to provide internal support (Fig. 7(b, c)). In such cases, the evolving front utilises the full range of operations: booleans, blends and trims (Fig. 8 (a)). The input primitive fields for these operations are generated by first extracting an oriented sub-graph from edges that meet at a node. This sub-graph is projected onto the ground-plane to get a 2D skeletal graph, which is subsequently used to generate the primitive fields (Fig. 8(b, c)).

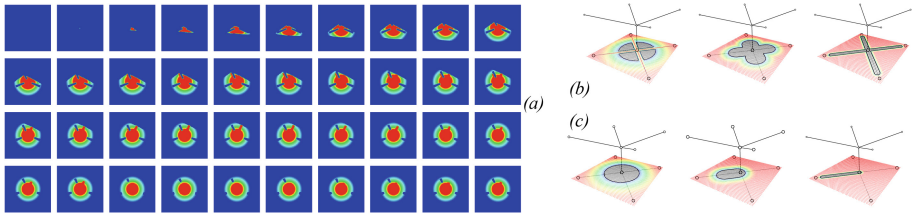


**Fig. 8.** (a) Secondary composite primitives formed by Boolean operations on primary primitives (b). (b) Primary primitive scalar fields generated as SDFs in relation to the vertices and edges.

## 4 Robotic 3D Printing

The conversion of the task graphs generated using the procedures previously described (Sect. 3.3) into motion instructions for the robot uses industry-standard procedures. The only significant geometric detail worth mentioning is that consecutive layers of task graphs need to be assembled into a single tool path. This involves first ensuring that the end of one layer and the start of the next are in proximity and subsequently adding a segment that will carry the print head smoothly across layers (Fig. 9).

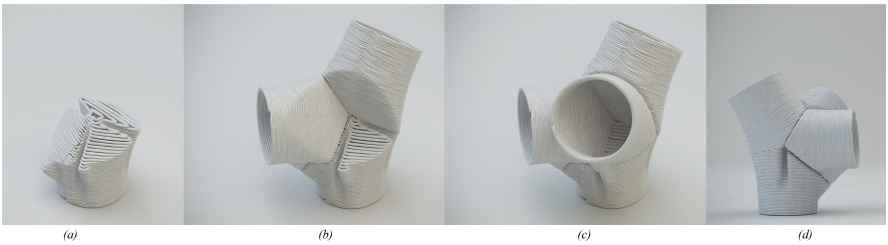


**Fig. 9.** Computer generated images show (a–c) printing sequence of the constituent parts of a node and (b) end result highlighting the groove feature that adds internal support to the print.

### 4.1 Path Planning

In current work, the bounding volumes of the each of the nodes is well within the operating sphere of the robot used. Further, the dimensions of the print head and apparatus in relation to the size of the print are also such that the need for extensive collision avoiding path planning is not necessary. However, we simulate and visually inspect the entire print trajectory of the robot along with the print head to ensure there are no collisions, particularly of the print head with the ground (Fig. 10).

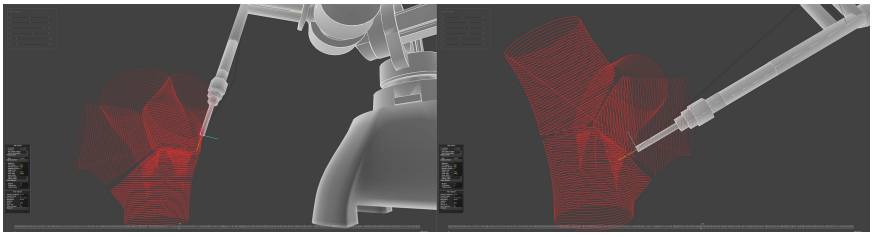

**Fig. 10.** Print trajectories and visual inspection of potential collision of print head with the already printed parts and/or the ground

### 4.2 Results

All results use C25 concrete (Fig. 11). The print duration for each of the prints is approximately 30 min and each segment of the nodes typically consists of 90–100

**Fig. 11.** Photographs showing materially bonded node parts (a, b) and the various types of nodes that vary in valence and angles between incident edges (c).

layers of 4 mm each. The diameter of each of the node segments is approximately 15 cm.

## 5 Future Work

The current proof-of-concept implementation of FRep for the shape design and its processing for fabrication of robotic 3D Printed concrete demonstrates the novelty and utility of the proposed framework. However, we envisage the following significant avenues of further investigation in the immediate future. Each of the avenues, we believe, are critical to the full-scale realisation of spatial structures: (1) Evolution of the front subject to constraints to ensure the shapes are guaranteed to be stable during print (Bhooshan et al. 2018). Current work circumvents this constraint by using very conservative layer height and overhangs; (2) Automated, structurally informed segmentation of skeletons larger than the print volume. In this regard, the formulation and modelling of equilibrium of rigid-block assemblies would be an important consideration (Frick et al. 2015); (3) Automatic insertion and growth of brackets at nodes that exceed allowed overhang angle; (4) Automatic inclusion of features to enable and ease fixings.

## 6 Conclusions

The current shape-design and physical results, whilst being early, already demonstrate the following: (1) Adaptation of skeleton-based FRep modelling for shape design for robotic 3D printing of concrete; (2) The subsequent adaptation of FRep to generate and represent tool-paths in robotic 3D printing; (3) First proof-of-concept implementation, opening further possibilities of adapting more sophisticated features from FRep and initial value formulation of front propagation. In particular, the mathematical framework of front propagation that can handle constrained evolution of the front, can be expected to be essential in handling several process and stability related constraints; (4) Potential for translating the proposed method as novel and alternative method of generating geometries of unreinforced, masonry.

In conclusion, the proposed use of a FRep shape representation schema as an alternative to ubiquitous BRep schemes is already providing novel results whilst easing fabrication-related post-production. We believe that this initial work will provide a strong foundation for exploring the design aspects of large-scale concrete printing, the unified representation of design and fabrication related parameters and thus the development of a novel architectural language of concrete extrusion.

## References

Bhooshan, S., Van Mele, T., Block, P.: Equilibrium-aware shape design for concrete printing. In: De Rycke, K., Gengnagel, C., Baverel, O., Burry, J., Mueller, C., Nguyen, M.M., Rahm, P., Thomsen, M.R. (eds.) Humanizing Digital Reality, Design Modelling Symposium 2017, pp. 493–508. Springer, Singapore (2017)

Bloomenthal, J., Bajaj, C.: Introduction to Implicit Surfaces. Morgan Kaufmann, San Francisco (1997)

Bloomenthal, J., Shoemake, K.: Convolution surfaces. In: Proceedings of the 18th Annual Conference on Computer Graphics and Interactive Techniques (ACM SIGGRAPH 1991), pp. 251–256. Las Vegas (1991)

Cacace, S., Cristiani, E., Rocchi, L.: A level set based method for fixing overhangs in 3D printing. Appl. Math. Model. **44**, 446–455 (2017)

Cohen, L.D.: On active contour models and balloons. CVGIP Image Underst. **53**, 211–218 (1991)

Desbrun, M., Gascuel, M.-P.: Animating soft substances with implicit surfaces. In: Proceedings of the 22nd Annual Conference on Computer Graphics and Interactive Techniques (ACM SIGGRAPH 1995), pp. 287–290. Los Angeles, CA (1995)

Frick, U., Van Mele, T., Block, P.: Decomposing three-dimensional shapes into self-supporting, discrete-element assemblies. In: Thomsen, M., Tamke, M., Gengnagel, C., Faircloth, B., Scheurer, F. (eds.) Modelling Behaviour, Design Modelling Symposium 2015, pp. 187–201. Springer, Cham (2015)

Hubert, E., Cani, M.-P.: Convolution surfaces based on polygonal curve skeletons. J. Symb. Comput. **47**, 680–699 (2012)

Ji, Z., Liu, L., Wang, Y.: B-Mesh: a modeling system for base meshes of 3D articulated shapes. In: Computer Graphics Forum, pp. 2169–2177. Wiley Online Library (2010)

Kass, M., Witkin, A., Terzopoulos, D.: Snakes: active contour models. Int. J. Comput. Vis. **1**, 321–331 (1988)

Keeter, M.: Hierarchical volumetric object representations for digital fabrication workflows. In: Proceedings of the 40th Annual Conference on Computer Graphics and Interactive Techniques (ACM SIGGRAPH 2013), Poster, Anaheim, CA (2013)

Lu, L., Sharf, A., Zhao, H., Wei, Y., Fan, Q., Chen, X., Savoye, Y., Tu, C., Cohen-Or, D., Chen, B.: Build-to-last: strength to weight 3D printed objects. ACM Trans. Graph. **33**, 97 (2014)

Monreal, A.: T-Norms, T-Conorms, aggregation operators and Gaudí's columns.In: Seising, R., González, V.S. (eds.) Soft Computing in Humanities and Social Sciences, pp. 497–515. Springer, Berlin, Heidelberg (2012)

Pasko, A., Adzhiev, V.: Function-based shape modeling: mathematical framework and specialized language. In: Winkler, F. (ed.) ADG 2002: 4th International Workshop on Automated Deduction in Geometry, Hagenberg Castle, Austria, pp. 132–160. Springer, Heidelberg (2002)

Perugini, P., Andreani, S.: Pier Luigi Nervi's columns: flow of lines and forces. J. Int. Assoc. Shell Spat. Struct. **54**, 137–148 (2013)

Popescu, M., Rippmann, M., Van Mele, T., Philippe, B.: Complex concrete casting: knitting stay-in-place formwork. In: Proceedings of the IASS 2016 Annual International Symposium: Spatial Structures in the 21st Century, Tokyo, p. 1278 (2016)

Rian, I.M., Sassone, M.: Tree-inspired dendriforms and fractal-like branching structures in architecture: a brief historical overview. Front. Archit. Res. **3**, 298–323 (2014)

Rossignac, J.: Blending and offsetting solid models Ph.D. thesis, University of Rochester (1985)

Sethian, J.: Fast marching methods and level set methods for propagating interfaces. In: Comput. Fluid Dyn. Annu. Lect. Ser. 29th, Rhode-Saint-Genese, Belgium (1998)

Sherstyuk, A.: Interactive shape design with convolution surfaces. In: Proceedings of the International Conference on Shape Modeling and Applications, Shape Modeling International 1999, pp. 56–65. Aizu-Wakamatsu, Japan (1999a)

Sherstyuk, A.: Kernel functions in convolution surfaces: a comparative analysis. Vis. Comput. **15**, 171–182 (1999)

West, M.: Fabric-formed concrete structures. In: Proceedings of First International Conference on Concrete and Development, pp. 133–142. Tehran, Iran (2001)

West, M.: The Fabric Formwork Book: Methods for Building New Architectural and Structural Forms in Concrete. Routledge, Abington, OX (2016)

Wyvill, B., Wyvill, G.: Field functions for implicit surfaces. Vis. Comput. **5**, 75–82 (1989)

Wyvill, G., McPheeters, C., Wyvill, B.: Soft objects. In: Kunii, T. (ed.) Advanced Computer Graphics: Proceedings of Computer Graphics Tokyo 1886, pp. 113–128. Springer, Tokyo (1986)

XtreeE (2017). Post in Aix-en-Provence. http://www.xtreee.eu/post-in-aix-en-provence/. Accessed 3 Sept 2018

Zastavni, D.: The structural design of Maillart's Chiasso Shed (1924): a graphic procedure. Struct. Eng. Int. **18**, 247–252 (2008)